Large-scale thermochemistry calculations for combustion models

Kiran K. Yalamanchi[*1], Yang Li[1,2], Tairan Wang[1], M. Monge-Palacios[1], S. Mani Sarathy[*1]

[1]King Abdullah University of Science and Technology (KAUST), Clean Combustion Research Center, Physical Sciences and Engineering Division, Thuwal, Saudi Arabia
[2]Science and Technology on Combustion, Internal Flow and Thermostructure Laboratory, School of Astronautics, Northwestern Polytechnical University, Xi'an 710072, China
*corresponding author email: kiran.yalamanchi@kaust.edu.sa; mani.sarathy@kaust.edu.sa

Abstract:

Accurate thermochemical properties for chemical species are of vital importance in combustion research. Empirical group additivity approaches are extensively used to generate thermochemistry data used in chemical kinetic models, but the accuracy is limited. In this work, we performed electronic structure calculations to determine reliable thermochemistry data for an extensive set of molecules that were taken from a large and well-established chemical kinetic model. The developed database consists of 1340 species that contain up to 18 and 5 carbon and oxygen atoms, respectively. The M06-2X/aug-cc-pVTZ level of theory was used for the geometry optimizations, vibrational frequency calculations, and dihedral angle scans. The potential energy of the different species was further refined with different composite methods, and the G3 method, together with the atomization reaction approach, was selected to calculate the enthalpy of formation at 0 K. This information was then used in statistical thermodynamics to calculate standard enthalpies of formation and entropy, as well as heat capacities at different temperatures. Our thermochemistry data exhibit good agreement with existing values in the literature, verifying the accuracy of our approach. The group additivity (GA) method is also examined based on the calculated values and significant differences are found, which indicates that GA values of relevant functional groups need to be updated. The database of thermochemistry quantities developed in this study is of particular interest not only for the update of GA values, but also to develop machine learning models for predicting the data of new species, which can assist in the development of combustion models. The impact of the developed dataset is illustrated by examining the variation in ignition delay times with the updated thermochemistry values.

1. Introduction:

Chemical kinetic models have played a crucial role in advancing the field of combustion. The necessity of detailed models for better accuracy has resulted an increase in the number of models over the last few decades [1]. However, obtaining the necessary thermochemistry and kinetics data from either experiments or electronic structure calculations for these models can be difficult, or even prohibitive. This has led to the development of approximated methods for determining necessary data, such as rate rules, group additivity (GA), and various correlations for species transport for the estimation of, respectively, rate constants, thermochemistry, and transport properties. Nevertheless, due to the tremendous increase in the computer power experienced in the last years, high level electronic structure calculations have become feasible for large species with numerous heavy atoms. Thus, more accurate data from density functional theory or even quantum chemistry methods is being currently generated, resulting in more accurate models and also in the improvement of estimation methods such as GA.

Accurate thermochemistry is critical to combustion simulations as the dependency of simulations on thermochemistry is two-fold. First, the temperature change in combustion simulations is computed from the difference in enthalpies of the species present in consecutive simulation steps. In addition, the standard practice followed by combustion modelers in order to maintain thermochemistry consistency within a chemical kinetic mechanism is to provide the rate coefficient of a given reaction for the forward direction, and then compute those for the reverse direction by using the former ones and the equilibrium constants that were obtained from thermochemistry. Therefore, the reaction coefficients of half of the reactions in a kinetic model effectively depend on thermochemistry. As an example, a change in the Gibbs free energy of 10 kcal mol^{-1} (or a change in entropy of 10 cal mol^{-1} K^{-1} not changing enthalpy) at 1000 K would result in a change of the reverse rate coefficient by a factor of 150. This highlights the necessity of determining thermochemical properties as accurately as possible.

Table 1: Thermochemical datasets containing a large set of species of interest in combustion.

Reference	Type	Year
Pedley et al. [2]	Indirect estimations from experiments	1986
DIPRR [3]	Compilation	2003

Yaws Handbook [4]	Compilation	2003
Baulch et al. [5]	Compilation	2005
CRC Handbook [6]	Compilation	2005
PrIMe [7]	Compilation	2007
TMTD [8]	Compilation	Continuously updated
NIST [9]	Compilation	Continuously updated
ATcT [10]	Thermochemical Network	Continuously updated
Goldsmith et al. [11]	RQCISD(T)/cc-PV∞QZ//B3LYP/6-311++G(d,p)	2012
Ghahremanpour et al. [12]	G2,G3,G4,CBS-QB3,W1U and W1BD	2016

Several databases that cover a large number of compounds of interest in combustion simulations are shown in Table 1. Most of the databases are a compilation from various sources, making the errors pass on from one source to another, and therefore not even systematic. In addition, most of these databases only provide data for standard enthalpy and entropy, excluding heat capacities. Goldsmith et al. [11] is the only database in Table 1 that contains values for the three thermodynamic functions and is not a compilation. It consists of 219 small molecules relevant in combustion chemistry, including species with different electronic configurations such as radicals and biradicals. There are several other works that published accurate thermochemistry data for species of interest in combustion by means of electronic structure calculations [13–21]. However, all of these works addressed only few types of species, and few of them were developed primarily for improvising the group values of the GA method. Moreover, the species contained in the above described datasets still represent a small portion of all the species that are present in the typical mechanism for combustion simulations of real fuel surrogates.

In recent years, the machine-learning (ML) technique has been proven to be a better alternative to GA methods in the prediction of accurate thermochemistry data [22–24]. However, ML models require a much larger database than GA methods to achieve a certain level of accuracy. In addition, unlike compilations, ML models need all the species to be addressed with the same methods in order to achieve a good performance. Therefore, with the goals of facilitating the implementation of ML models for combustion applications and improve kinetic models performance, a consistent

thermochemistry database for a large number of species is developed in this work. The considered species are closed-shell species from the Co-optima mechanism [25,26], making sure that the database spans across all the kinds of hydrocarbons in typical chemical kinetic mechanisms. In this work, we focused on stable species rather than on radicals. However, the thermodynamic functions of the corresponding radical species can be computed from those of the corresponding closed shell species and the bond energy of the broken bond by using similar methods to those adopted by GA. Nevertheless, a similar database to that obtained in this work but for radical species would be advantageous for a more accurate description of their thermochemistry.

In this work, electronic structure calculations combined with statistical thermodynamics are used to compute the thermodynamic properties of 1340 species consisting of C, H and O atoms. The M06-2X [27] method and aug-cc-pVTZ [28] basis set were used for the optimization, characterization, and dihedral angle scans to include torsional anharmonicity, of the stationary points; the zero kelvin energies (ZKE), or zero point energy corrected energies, were further refined with the CBS-APNO [29], G3 [30], and G4 [31] composite methods. The accuracy of the three composite methods was assessed by comparison to ATcT values [10], the one with the best performance was selected, and the corresponding computed thermochemistry values are then compared with literature values and group additivity methods.

2. Methods and Procedure:

2.1. Selection of Species:

The species investigated in this work were taken from the Co-optima mechanism [25,26], the latest model of the which is C3MechV3.3 [32]. This mechanism is selected for its detailed chemistry to describe a wide range of species of importance in combustion simulations. The fuel components for which sub-mechanisms are available in the mechanism are shown in Table 2. This includes alcohols from methanol to pentanol, C5 cyclic species, A1 and A2 aromatics, acetates, ethers, ketones, aldehydes and furans. The majority of the reactions included in the mechanism are those describing the combustion kinetics of C1-C8 alkanes, alkenes and alkynes. The mechanism has a total of 3701 species, consisting of closed shell species and radicals, some of them compounds with atoms other than carbon, hydrogen and oxygen.

Table 2: Summary of sub mechanisms implemented in the Co-optima mechanism.

Alcohols	**Paraffins**	**Unsaturates**	**Cyclic & Aromatics**	**Other Species**
Methanol	Methane	Ethene	Cyclopentane	Methyl Acetate
Ethanol	Ethane	Acetylene	Cyclopentanone	2-Butanone
N-Propanol	Propane	Propene	Cyclopentadiene	Ethyl Acetate
Iso-Propanol	Butane	Allene	Benzene	2-Methylfuran
N-Butanol	N-Pentane	Propyne	Phenol	Methyl Butanoate
2-Butanol	Iso-Pentane	1-Butene	Toluene	2,5-Dimethylfuran
Iso-Butanol	N-Hexane	2-Butene	Ethyl Benzene	Anisole
Tert-Butanol	2-Methylhexane	Iso-Butene	Ortho-Xylene	Formaldehyde
N-Pentanol	N-Heptane	1,3-Butadiene	Para-Xylene	Dimethyl Ether
Iso-Pentanol	Iso-Octane	1-Pentene	1,2,4-Trimethylbenzene	Acetaldehyde
2-Methyl-1-Butanol		2-Pentene		
		1-Hexene	1,3,5-Trimethylbenzene	
		2-Hexene		
		3-Hexene	Alpha-Methylnaphthalene	
		2,4,4-Trimethylpent-2-Ene		
		2,4,4-Trimethylpent-1-Ene		

For this work, closed shell species with only carbon, hydrogen, and oxygen atoms from the Co-optima mechanism were considered. There are 1368 such species in the mechanism, whose maximum number of carbon and oxygen atoms is 18 and 5, respectively. Figure 1 provides an overview of the size, defined as per the number of carbon atoms, of the species investigated in this work. Species with 5, 6, and 7 carbon atoms are the most prominent ones in our dataset and account for about 72% of the total species. Although the maximum carbon atom number in the dataset is 18, the total number of species with more than 9 carbon atoms are only 23 and account for only 1.5%.

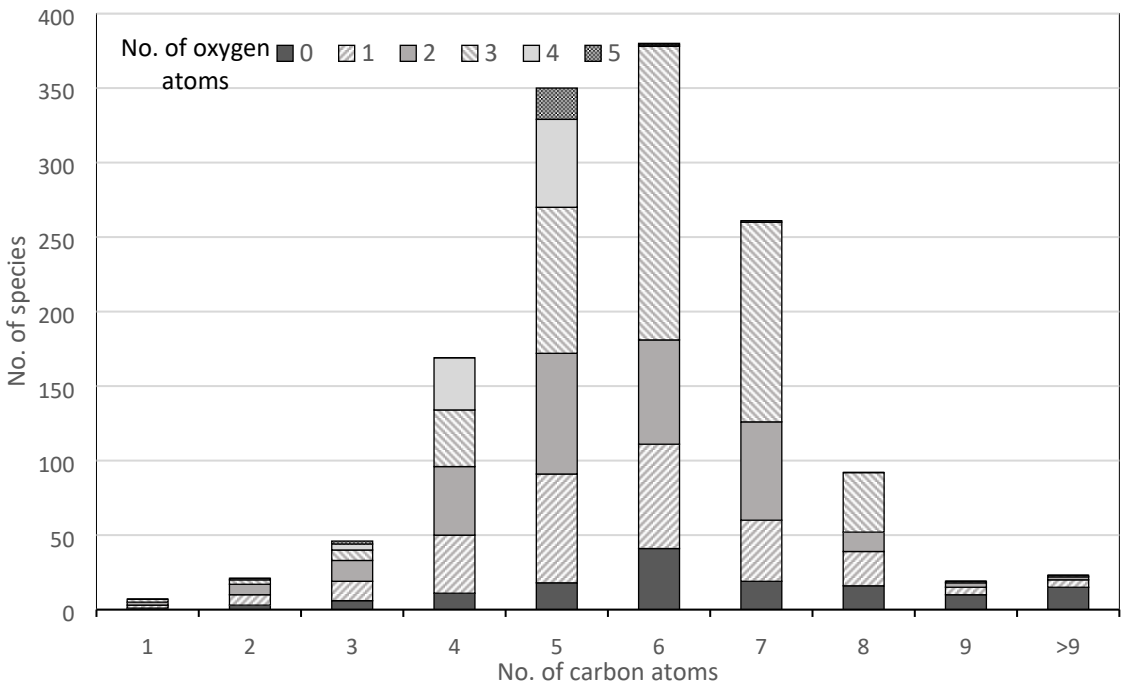

Figure 1: The proportion of different species kinds in terms of the number of carbon and oxygen atoms.

From Fig. 1, it can be also observed that most of the species are oxygenates primarily representing the mechanism's low temperature chemistry. Oxygenates constitute 90% of the dataset and an overview of the species within each category of oxygenates is shown in Figure 2. There are only 140 non-oxygenated species, and those with more than 8 carbon atoms are all cyclic species. The 278 species with one oxygen atom are C1-C5 alcohols, ketones, aldehydes, and five-membered rings formed from radical peroxide species, among others. There are 304 species with two oxygen atoms, and the majority of these are hydroperoxides. The 521species with three oxygen atoms are primarily keto-hydroperoxides species that take part of the degenerate branching path in low temperature chemistry. The increasing number of species as the number of oxygen atoms is increased from 0 to 3 is due to the increasing number of possible combinations in which those oxygen atoms can be attached to the carbon chain. In addition, there are 101 species with four oxygen atoms, which are majorly di-peroxides, and 24 with 5 oxygen atoms.

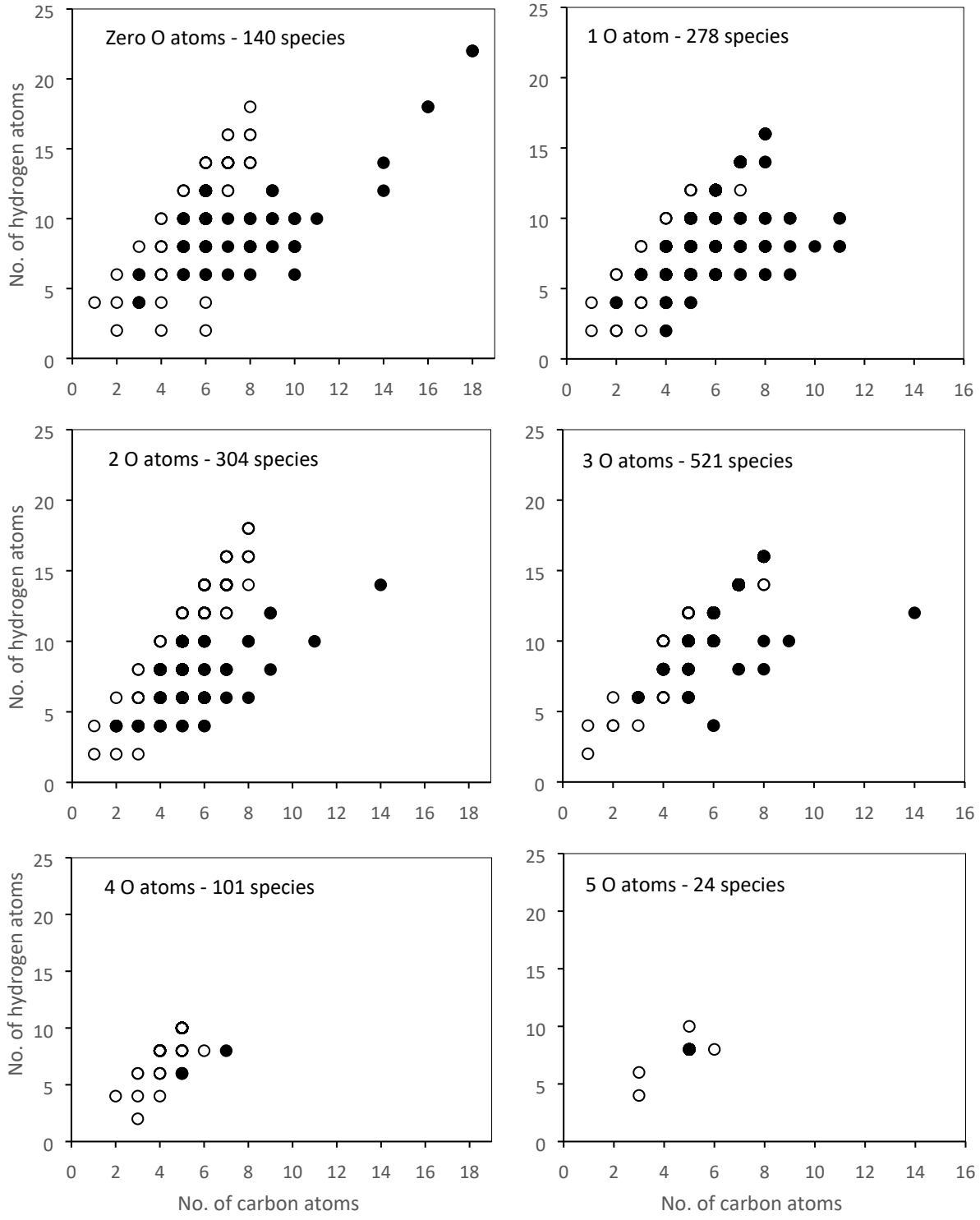

Figure 2: C/H ratio of the compounds present in the dataset for different oxygenates. The filled circles indicate that there are cyclic structures for that C/H ratio.

2.2 Electronic Structure Calculations:

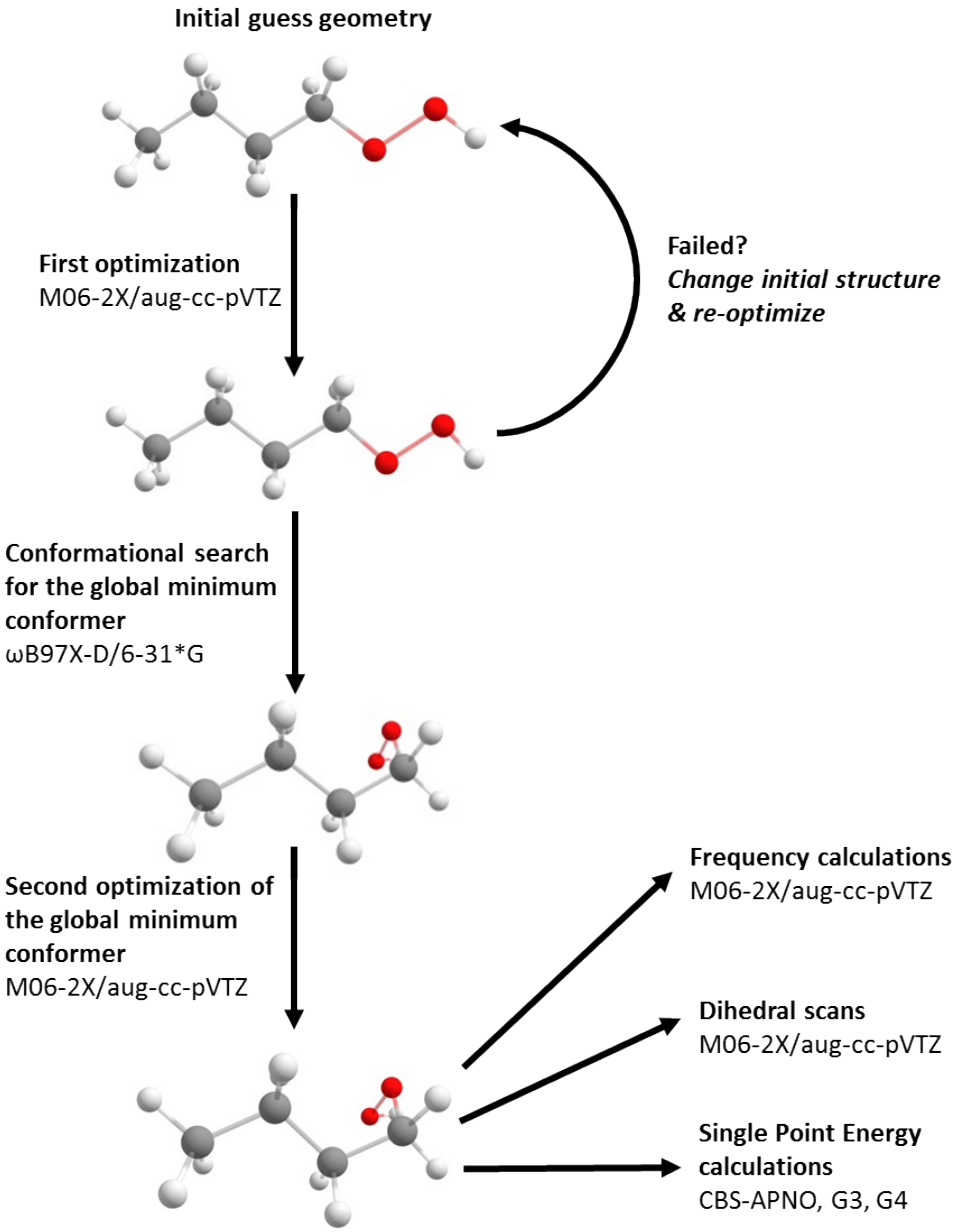

Figure 3: Workflow of the electronic structure calculations performed in this work for obtaining the required data to compute the thermochemical properties.

For the selected 1368 species, electronic structure calculations were performed to obtain their gas phase enthalpy of formation and entropy at standard conditions, as well as their heat capacities for a range of temperatures. The geometry, vibrational frequencies, and ZKE of the species are necessary to calculate their thermodynamic functions, and Figure 3 shows the workflow followed

in this work to obtain them. The first step of the workflow is to obtain a guess 3-D geometry for each of the 1368 species, which are obtained from the website https://cactus.nci.nih.gov/translate/ by providing the SMILES (Simplified Molecular Input Line Entry System) strings of the species; 3D atomic coordinates are computed by the algorithm of the CORINA program in the website.

The initial guess geometries were first optimized using the M06-2X/aug-cc-pVTZ level of theory, and the functional M06-2X was selected for its good performance in thermochemistry. Whilst the majority of the species were successfully optimized, the optimization of about 5% of them failed. For these species, the initial guess geometry was modified until a successful optimization was achieved. The conformational space of the first optimized conformer of each species was screened by rotating all the dihedral angles every 120 degrees and by optimizing the generated conformers with the goal of finding the lowest potential energy conformer or global minimum. Since numerous conformers were generated for each species, a more affordable level of theory, which consists of the ωB97X-D [33] method and the smaller basis set 6-31*G [34,35], was used for the global minimum search. We are aware that a smaller basis sets may result in larger errors; however, the relative energies predicted by both levels of theory are likely very similar. All the global minima conformers that were identified by the low level optimization were further subjected to a second optimization using the M06-2X/aug-cc-pVTZ in order to yield more accurate thermochemical data.

Using the same level of theory, that is, M06-2X/aug-cc-pVTZ, the final optimized global minima were then characterized by calculating their vibrational frequencies, and their dihedral angles were scanned in order to implement torsional anharmonicity corrections; furthermore, their ZKE were calculated by conducting single point energy calculations with the composite methods CBS-APNO, G3 and G4. These composite methods were selected based on the study by Somers et. al. [36,37], who investigated the performance of several composite methods and concluded that the average values from those three reproduced with more fidelity the benchmark results. All the electronic structure calculations, except the conformal analysis, were performed using the Gaussian 16 software [38] in KAUST supercomputing clusters IBEX and Shaheen. The conformal analysis is performed using Spartan'18 software [39] on a Supermicro SYS7049A-T workstation.

2.3. Methods for the Determination of the Enthalpies of Formations at 0 K:

There are two methods that can be employed to calculate the enthalpy of formation at 0 K ($\Delta_f H_0$) of the species from their ZKE, i.e. isodesmic and atomization methods. In the isodesmic method, for a given species, a balanced reaction is built so that the numbers of chemical bonds of each type are the same on both sides of the reaction. The $\Delta_f H_0$ is then determined on the basis of the heat of reaction and the standard formation enthalpies of the reactants and products involved in the reaction.

The atomization method considers a molecule to be formed from its constituent atoms for calculating its $\Delta_f H_0$, as shown in Equation 1. The theoretical atomization energy at 0 K (TAE_0) is therefore calculated for the species C_xH_y using Equation 2, where H_0 is the ZKE calculated using each composite method. Thereafter, the enthalpy of formation of C_xH_y ($\Delta_f H_0$) can be calculated from TAE_0 and the standard formation enthalpies of the component atoms in their gaseous state, as shown in Equation 3.

$$xC + yH \rightarrow C_xH_y \quad \ldots\ldots\ldots\ldots (1)$$

$$TAE_0 = x\,H_0(C) + y\,H_0(H) - H_0(C_xH_y) \quad \ldots\ldots\ldots\ldots\ldots (2)$$

$$\Delta_f H_0(C_xH_y) = x\,\Delta_f H_0(C) + y\,\Delta_f H_0(H) - TAE_0 \ldots\ldots\ldots\ldots\ldots (3)$$

Although both methods should yield the same results in theory, some differences will be observed due to the different reference chemical data considered by each of them. However, even for practical considerations, both methods have shown to yield similar results [13]. The isodesmic method involves manually building isodesmic reaction pathways for each of the species in the dataset, which is not always straightforward. On the other hand, the atomization method is simpler to scale for large datasets such as that in this study. Therefore, the atomization method was adopted for this study, and the reference standard formation enthalpies of the component atoms were taken from the ATcT tables as shown in Table 3.

Table 3: Gaseous atomic formation enthalpies at 0 K taken from the ATcT dataset (kcal mol^{-1})

T/K	C (^3P)	H ($^2S_{1/2}$)	O (^3P)
0	170.03	51.63	59.00

2.4. Statistical Thermodynamics- Standard Enthalpies and Entropies and Heat Capacities:

The vibrational frequencies and dihedral scans of the optimized geometries obtained with the M06-2X/aug-cc-pVTZ level of theory, together with the enthalpies of formation at 0 K ($\Delta_f H_0$) calculated with the selected composite method, were used as input to the MultiWell program suit [40] to calculate, using statistical thermodynamics, the enthalpies of formation and entropies at 298.15 K as well as the temperature-dependent heat capacities.

The dihedral scans were used to account for the effects of torsional anharmonicity associated to the lower-frequency modes by using the hindered rotor approximation. In addition, our vibrational frequencies were scaled by using the scaling factor reported in previous works for the M06-2X/aug-cc-pVTZ level of theory; the goal of this frequency scaling was not only to further improve the description of torsional anharmonicity in low-frequency modes, but also to improve the description of this effect in higher-frequency modes and derive more accurate ZKE values. Two different frequency scaling factors have been reported for the M06-2X/aug-cc-pVTZ level of theory, one the NIST database [9] and another one by Alecu et al. [41]; the latter [41] recommends a value of 0.985, while the former [9] recommends 0.956. Our choice was based on the comparison of the values of the enthalpy of formation at 298.15 K ($\Delta_f H_{298}$) derived from using both scaling factors with the values from the ATcT tables, discussed in section 3.1.

3. Results and discussion:

3.1 Enthalpies of Formation at 0 K:

The derived enthalpies of formation at 0 K ($\Delta_f H_0$) with the CBS-APNO, G3 and G4 composite methods, using the atomization method as described in section 2.3, were compared against the values from the ATcT tables. The ATcT tables are built in such a way that its thermochemistry data is internally consistent, and results in one of the most reliable sources of thermochemistry data. However, many of the species that are relevant in combustion chemistry are not described in those tables, and in fact, among the 1368 species considered in our study, only 60 are available in the ATcT tables. Table 4 shows the comparison of the values of $\Delta_f H_0$ predicted by the composite methods CBS-APNO, G3, and G4 used in this study with those by the ATcT tables for the 60 available species. The mean absolute error relative to the ATcT tables for CBS-APNO, G3, and G4 is, respectively, 1.58, 0.39 and 0.37 kcal mol^{-1}. G3 and G4 methods exhibit better agreement

with the ATcT results, and even the average values from the CBS-APNO, G3 and G4 predictions, as suggested by Somers et al. [36,37], have a larger error of 0.65 kcal mol^{-1} due to the relatively large deviation of the CBS-APNO method. The missing values in Table 4 for the G4 method are due to the convergence error in the self-consistent field algorithm that was encountered in the calculation of the single point energies. Comparing the mean absolute errors for only those species for which the G4 method converged, G3 and G4 have both an error of 0.37 kcal mol^{-1}. Therefore, the G3 method is used in this study to calculate our final thermochemical data as it converged for the majority of the species.

The largest deviation between the ATcT and composite methods predictions is observed for peroxyformic acid (species no. 60 in Table 4), with a difference of 3.77 kcal mol^{-1} between the ATcT and G3 methods. However, the difference between ATcT and G3 values is greater than 1 kcal mol^{-1} for only two other species, cyclopentadiene and 1,3-butadiyne (species no. 21 and 40, respectively, in Table 4). For the remaining 57 species, the average difference is 0.30 kcal mol^{-1}, which suggests that the $\Delta_f H_0$ values calculated with the G3 method are in good agreement with those from the ATcT tables.

Table 4: Comparison of the $\Delta_f H_0$ values calculated with the CBS-APNO, G3 and G4 composite methods used in this study and the ATcT Tables (kcal mol^{-1}). The average value obtained from the three composite methods is also compared.

No	Species	ATcT	CBS-APNO	G3	G4	Average
1	Methane	-15.91	-16.94	-16.20	-15.92	-16.35
2	Ethane	-16.34	-17.92	-16.52	-16.09	-16.85
3	Ethylene	14.55	14.29	14.48	14.54	14.44
4	Methanol	-45.42	-46.23	-45.42	-45.38	-45.68
5	Formaldehyde	-25.19	-25.58	-25.61	-25.82	-25.67
6	Propane	-19.78	-21.88	-19.83	-19.32	-20.34
7	Ethanol	-51.94	-53.20	-51.88	-51.62	-52.23
8	Acetylene	54.69	55.83	55.19	54.78	55.27
9	Propene	8.35	7.50	8.49	8.60	8.20
10	Benzene	24.05	21.99	24.82		23.41
11	Acetaldehyde	-37.07	-37.98	-37.21	-37.16	-37.45
12	n-Butane	-23.53	-26.05	-23.39	-22.85	-24.10
13	Propyne	46.07	45.79	46.31	46.08	46.06
14	Ketene	-10.84	-11.27	-11.26	-10.87	-11.14
15	Toluene	17.52	14.60	17.94		16.27
16	1,3-Butadiene	29.95	29.87	30.34	30.25	30.15

17	Phenol	-17.84	-20.00	-17.27		-18.63
18	Acetic acid	-100.11	-101.00	-100.05	-99.64	-100.23
19	Allene	47.16	46.95	47.00	47.11	47.02
20	Methyl hydroperoxide	-27.47	-28.10	-27.00	-27.27	-27.45
21	Cyclopentadiene	36.11	35.43	37.21		36.32
22	Methoxymethane	-39.78	-41.53	-40.07	-39.86	-40.49
23	Cyclopropane	16.96	15.69	17.65	17.19	16.85
24	Isobutene	0.96	-0.43	1.29	1.35	0.74
25	1-Butene	5.02	3.91	5.52	5.77	5.07
26	n-Pentane	-27.34	-30.24	-26.97		-28.61
27	Cyclopropene	69.84	69.86	70.71	70.17	70.25
28	n-Hexane	-31.08	-34.48	-30.60		-32.54
29	Benzaldehyde	-4.63	-7.01	-4.50		-5.76
30	Cyclopentane	-10.49	-13.24	-10.14		-11.69
31	2-Butyne	38.09	37.22	38.29	38.36	37.96
32	Isoprene	22.97	22.28	23.48		22.88
33	Ethynol	22.82	23.28	22.93	22.91	23.04
34	Glyoxal	-49.65	-50.09	-50.10	-50.33	-50.17
35	Propionaldehyde	-40.96	-42.28	-40.90	-40.70	-41.29
36	trans-2-Butene	2.24	0.83	2.57	2.73	2.04
37	iso-Pentane	-28.48	-31.57	-28.35		-29.96
38	neo-Pentane	-32.18	-35.21	-32.06		-33.63
39	1-Butyne	42.91	42.56	43.43	43.35	43.11
40	1,3-Butadiyne	109.42	110.45	110.50	109.62	110.19
41	Ethylbenzene	13.90	10.30	14.21		12.81
42	Phenylethene	40.55	38.57	41.42		39.99
43	Phenylacetylene	79.45	77.43	80.21		78.82
44	1,2-Butadiene	42.01	41.26	42.04	42.18	41.83
45	Cyclohexane	-19.97	-23.25	-19.72		-21.48
46	Methylketene	-13.07	-14.00	-13.28	-12.74	-13.34
47	n-Heptane	-34.81	-38.72	-34.24		-36.48
48	1-Propanol	-55.31	-57.18	-55.32	-54.90	-55.80
49	2-Propanol	-59.61	-61.54	-59.71	-59.18	-60.15
50	iso-Hexane	-32.18	-35.79	-31.98		-33.89
51	2-Butanone	-51.85	-53.98	-51.83		-52.91
52	2-Propynal	32.39	32.76	32.21	31.98	32.32
53	Anisole	-11.42	-14.35	-11.05		-12.70
54	Propionic acid	-104.30	-105.36	-103.85		-104.61
55	Acrolein	-13.22	-13.50	-13.30	-13.27	-13.36
56	Methyl formate	-82.90	-84.02	-83.31	-83.04	-83.46
57	Ethenol	-26.95	-27.43	-26.94	-26.75	-27.04
58	2,2,4-Trimethylpentane	-40.94	-46.25	-41.56		-43.91
59	3-Buten-2-one	-22.84	-23.87	-22.91		-23.39

60	Peroxyformic acid	-66.75	-63.55	-62.98	-63.08	-63.21
	Mean absolute error		**1.58**	**0.39**	**0.37**	**0.65**

For choosing between the two frequency scaling factors discussed in section 2.4, a Bland−Altman plot showing this comparison is shown in Fig. 4 for the species whose data is available in the ATcT tables. Both scaling factors yield similar $\Delta_f H_{298}$ values, which is mainly due to its negligible effect on the enthalpy at low temperatures. However, the mean absolute error for the Alecu et al. [41] scaling factor (0.34 kcal mol^{-1}) is marginally better than that of the NIST scaling factor (0.37 kcal mol^{-1}), and a detailed comparison is shown in the supplementary material. Therefore, the frequency scaling factor of 0.985 by Alecu et al. [41] was adopted in this study.

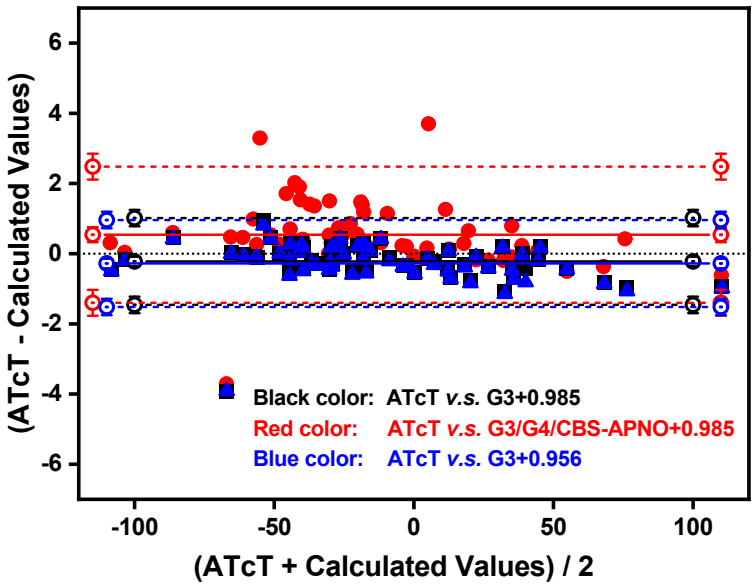

Figure 4: Comparison of the $\Delta_f H_{298}$ values derived using different composite methods and scaling factors with the values reported in the ATcT tables.

3.2 Standard Enthalpies, Entropies and Heat Capacities- Comparison with other Datasets and Group Additivity:

The standard enthalpy and entropy, as well as the heat capacity, of the investigated species were calculated using the enthalpies of formation at 0 K that were calculated with the M06-2X/aug-cc-pVTZ and G3 levels of theory using the 0.985 scaling factor, as was previously discussed.

Although ATcT thermochemical database is one of the most reliable sources of thermochemistry, it is limited to enthalpy of formations. Goldsmith et al. [11] calculated enthalpies, entropies, and heat capacities for C1-C4 species including many radicals and biradicals with the RQCISD(T)/cc-PV∞QZ//B3LYP/6-311++G(d,p) level of theory. To the best of our knowledge, this is the only prior work that published large-scale thermochemistry data of species relevant to combustion chemistry. Although Goldsmith et al. used geometries at the B3LYP/6-311++G(d,p) level of theory, they have adopted bond additivity corrections to match enthalpies with the ATcT database. A comparison of the values reported by this work, Goldsmith et al. [11] and NIST database [9] for the standard enthalpy, entropy and heat capacity at different temperatures is shown in Table 5 . It should be noted that the NIST database is a compilation of data from several works, and thus it may not be consistent for some species. In Table 5, a few of those species that are common in the three datasets that are compared are shown, and those include C1-C4 n-alkanes, C1-C3 n-alcohols and aldehydes.

Table 5: Comparison of the values reported by Goldsmith et al. [11] (GS), NIST database and this study (KAUST) for the standard enthalpy (kcal mol^{-1}) and entropy (cal mol^{-1} K^{-1}), and heat capacity (cal mol^{-1} K^{-1}) of some important species in combustion at different temperatures (K).

			$\Delta_f H^{\ominus}$	$S^{\ominus}$	C_p					
Species	Structure	Source	298	298	300	400	600	800	1000	1500 (K)
CH4	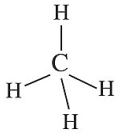	KAUST	-18.10	44.46	8.51	9.63	12.38	14.87	16.95	20.49
		GS	-17.60	44.40	8.50	9.60	12.40	14.90	17.00	20.50
		NIST	-17.81	45.09	8.55	9.71	12.61	15.32	17.63	21.72
C2H6	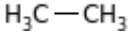	KAUST	-20.31	54.46	12.25	15.34	21.24	25.90	29.52	35.34
		GS	-20.00	54.70	12.60	15.50	21.10	25.50	29.00	34.60
		NIST	-20.03		12.60	15.65	21.32	25.80	29.29	34.87
C3H8		KAUST	-25.12	66.91	17.76	22.40	30.46	36.54	41.23	48.77

		GS	-25.20	66.10	17.80	22.40	30.50	36.60	41.30	48.90
		NIST	-25.02		17.67	22.47	30.76	36.99	41.73	49.21
		KAUST	-29.88	74.70	23.24	29.22	39.67	47.50	53.47	62.97
C4H10		GS	-30.00	73.70	24.00	29.70	39.90	47.70	53.70	63.10
		NIST	-30.02		23.65	29.82	40.46	48.37	54.34	63.67
		KAUST	-48.03	57.26	10.46	12.21	15.90	18.85	21.16	24.96
CH3OH	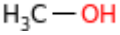	GS	-48.20	57.20	10.60	12.40	16.00	19.00	21.20	25.00
		NIST	-49.00		10.56	12.34	16.06	19.06	21.40	25.19
		KAUST	-56.08	67.30	15.67	19.15	25.34	29.95	33.47	39.17
C2H5OH		GS	-56.40	66.80	15.70	19.20	25.50	30.10	33.60	39.30
		NIST	-55.93		15.65	19.41	25.87	30.57	34.10	39.68
		KAUST	-60.99	75.00	21.18	26.43	35.36	41.82	46.66	54.34
NC3H7OH		GS	-61.30	76.30	20.90	25.90	34.60	41.00	45.90	53.50
		NIST	-61.19		20.54	25.82	34.75	41.26	46.12	53.76
		KAUST	-26.53	52.21	8.43	9.30	11.36	13.18	14.60	16.84
CH2O	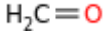	GS	-26.20	52.20	8.40	9.30	11.40	13.30	14.70	16.90
		NIST	-27.70	52.33	8.47	9.38	11.52	13.37	14.81	17.01
		KAUST	-39.76	62.70	13.31	16.01	20.88	24.59	27.39	31.75
CH3CHO		GS	-39.60	63.00	13.00	15.50	20.20	23.80	26.60	30.90
		NIST	-40.80		13.27	15.84	20.54	24.16	26.89	31.09
C2H5CHO		KAUST	-44.50	72.93	19.83	22.95	29.38	34.57	38.57	44.87

	GS	-45.00	73.50	18.90	22.40	29.20	34.60	38.60	44.90
	NIST	-45.10	72.75	19.35	23.04	30.71	37.09	42.14	50.60

The three sets of data compared in Table 5 are in good agreement. The mean absolute difference between the present work and that by Goldsmith et al. is 0.28 kcal mol^{-1} for $\Delta_f H_{298}$, 0.48 cal K^{-1} mol^{-1} for $S^{\ominus}_{298}$ and 0.26 cal K^{-1} mol^{-1} for C_p, and those between our work and the NIST database are 0.49 kcal mol^{-1} for $\Delta_f H_{298}$, 0.31 cal K^{-1} mol^{-1} for $S^{\ominus}_{298}$ and 0.54 cal K^{-1} mol^{-1} for C_p. The largest differences were observed for the high temperature heat capacities of propanal reported by the present work and the NIST database. Although Goldsmith et al.'s dataset is based on less accurate optimized geometries (B3LYP/6-311++G(d,p)) than our dataset (M06-2X/aug-cc-pVTZ), both are in good agreement due to the bond additivity corrections implemented in the former.

Benson group additivity is an easy and fast method for calculating thermochemistry properties. This method determines each of the thermochemistry properties by summing the contribution from the constituent groups present in a given species. Although corrections such as gauche interactions and symmetry corrections need additional inputs, GA is still a convenient method and has been widely used for generating thermochemistry data for the species in kinetic models. The group values have been constantly updated as more accurate data is developed over the years. The thermochemistry data for the set of species in the Co-optima mechanism generated with GA method with the most recent group values are available along with the mechanism. A comparison between all the data curated in this study and GA values would be unwieldy to present. For this reason, a comparison of a set of species that are involved in the chemistry of the iso-pentane fuel component is discussed in this section for the illustration of the accuracy of the widely used GA method.

Iso-pentane is an important fuel component whose combustion chemistry involves different kind of species whose thermochemistry has been assessed in our work. Some of those species are the four hydroperoxides that are formed from the corresponding four carbon distinct sites of iso-pentane, as well as ten keto-hydroperoxides species. Note that the corresponding radical's thermochemistry, i.e. hydroperoxyl and keto-hydroperoxyl radicals, was computed by the GA method from the thermochemistry of their corresponding closed shell species, and this makes the targeted species for the current comparison especially important. The comparison between the

thermochemistry values predicted by the GA method and our more robust approach is shown in Table 6.

Table 6: Comparison of the values reported with the GA method and by this study (KAUST) for the standard enthalpy (kcal mol^{-1}) and entropy (cal mol^{-1} K^{-1}), and heat capacity (cal mol^{-1} K^{-1}) of some important species involved in the combustion of iso-pentane at different temperatures (K).

			$\Delta_f H^{\ominus}$	$S^{\ominus}$	C_p					
Species	Structure	Source	298	298	300	400	600	800	1000	1500 (K)
IC5H12	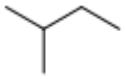	GA	-36.42	83.21	28.74	36.39	49.35	58.84	65.99	77.31
		KAUST	-36.33	82.48	29.26	37.30	50.06	59.48	66.57	77.59
AC5H11O2H	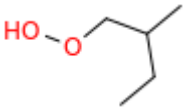	GA	-54.92	95.80	36.53	45.10	59.28	69.53	77.16	89.16
		KAUST	-54.94	102.37	36.43	45.41	59.36	69.35	76.67	87.80
BC5H11O2H	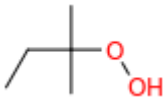	GA	-62.27	94.56	35.92	44.86	59.30	69.53	77.13	89.08
		KAUST	-63.29	95.25	37.47	46.14	59.61	69.31	76.49	87.53
CC5H11O2H	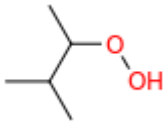	GA	-59.08	94.14	35.49	44.34	58.86	69.23	76.91	88.96
		KAUST	-58.96	98.75	37.69	46.56	60.12	69.66	76.59	87.35
DC5H11O2H	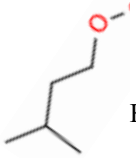	GA	-55.47	90.65	35.11	44.27	59.31	69.95	77.77	89.97
		KAUST	-54.94	101.00	36.43	45.41	59.36	69.35	76.67	87.80
IC5KETDB	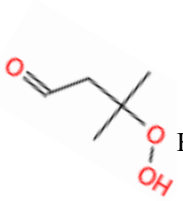	GA	-82.81	90.84	36.68	45.51	59.22	68.70	75.61	86.29
		KAUST	-83.03	100.96	37.87	45.94	58.59	67.67	74.23	83.77
IC5KETDA		GA	-78.72	92.51	35.04	43.98	58.44	68.55	75.86	86.99

	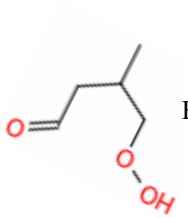	KAUST	-74.68	108.09	36.85	45.22	58.33	67.70	74.40	83.99
IC5KETAC	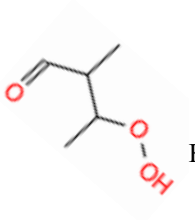	GA	-78.63	95.96	39.95	47.46	59.16	67.98	74.69	85.28
		KAUST	-78.93	106.40	37.64	45.73	58.98	68.80	75.78	85.13
IC5KETAA	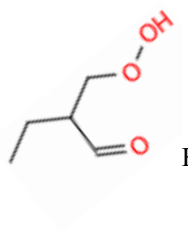	GA	-74.92	96.17	36.88	45.27	58.90	68.52	75.53	86.32
		KAUST	-74.91	108.66	36.92	44.90	57.64	66.97	73.77	83.68
IC5KETDC	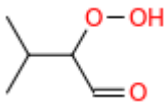	GA	-77.48	93.06	35.94	44.63	58.56	68.29	75.36	86.21
		KAUST	-75.39	107.69	37.88	47.51	61.63	70.90	77.13	85.76
IC5KETAD	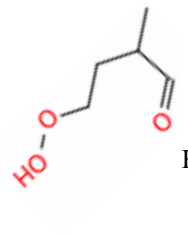	GA	-78.09	92.19	34.89	43.91	58.44	68.55	75.85	86.97
		KAUST	-74.91	108.66	36.92	44.90	57.64	66.97	73.77	83.68
IC5KETAB	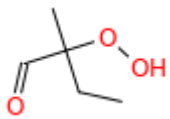	GA	-80.11	97.00	37.62	45.80	58.92	68.17	74.95	85.46
		KAUST	-77.77	106.96	38.20	47.33	61.23	70.75	77.29	86.13
IC5KETCA	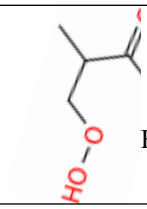	GA	-82.83	93.53	35.89	44.35	58.14	67.89	75.00	85.97
		KAUST	-83.18	108.31	36.67	44.24	56.40	65.40	72.08	82.19

IC5KETCB	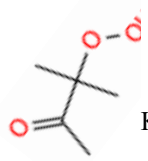	GA	-87.59	94.45	36.80	45.03	58.20	67.53	74.40	85.10
		KAUST	-86.04	105.25	37.93	46.66	60.01	69.23	75.63	84.55
IC5KETCD	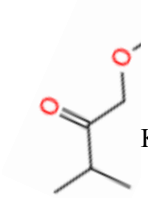	GA	-80.57	97.89	36.31	44.57	57.96	67.45	74.40	85.18
		KAUST	-79.63	109.12	37.30	46.13	59.50	68.45	74.95	83.91

The agreement between both approaches is remarkably good for the iso-pentane case, with $\Delta_f H_{298}$, $S^{\ominus}_{298}$, and C_p values within 0.1 kcal mol^{-1}, 1 cal K^{-1}mol^{-1} and 1 cal K^{-1}mol^{-1}, respectively. However, this is not the case for the oxygenated species. For the hydroperoxides, average differences of 0.42 kcal mol^{-1}, 5.56 cal K^{-1} mol^{-1} and 0.92 cal K^{-1} mol^{-1} for $\Delta_f H_{298}$, $S^{\ominus}_{298}$, and C_p for the different temperatures, respectively, are observed; for the keto-hydroperoxides case the agreement between both methodologies is even worse, and the corresponding average values are 1.5 kcal mol^{-1}, 12.65 cal K^{-1} mol^{-1} and 1.46 cal K^{-1} mol^{-1}.

The differences observed for the entropy thermodynamic function are especially pronounced, with differences of even 16.47 cal K^{-1} mol^{-1} for the species IC5KETAD. The GA method consistently under predicts the entropy of the oxygenated-derived species of iso-pentane. Moreover, although the $\Delta_f H_{298}$ average difference seems to be low, six among the fifteen oxygenated species have an enthalpy difference over 1 kcal mol^{-1}, with the largest deviation of 4.04 kcal mol^{-1} for the IC5KETDA case. Similarly, for heat capacities a difference of over 1 cal mol^{-1} K^{-1} is observed for many species at different temperatures, reaching a maximum discrepancy of 3.78 cal mol^{-1} K^{-1} for IC5KETCA at 1500 K. We attribute the observed deviations between both methods to, at least to some extent, the intramolecular hydrogen bonds that are present in the hydroperoxy and keto-hydroperoxy species since the GA method does not account for those interactions.

A detailed comparison of the performance of both methods for all the species of our database is out of the scope of this study. However, the previous illustration for iso-pentane and its derived hydroperoxy and keto-hydroperoxy species proves the potential of this work and its utility to update and improve the thermochemistry of current kinetic models.

3.3 Effect of the Updated Thermochemistry on the Performance of Kinetic Models:

The thermochemistry data in the Co-optima mechanism, which was generated with the GA method, was replaced with the data calculated in this study to assess the performance of the updated kinetic model. Therefore, the thermodynamic functions of 1340 out of the 3701 species described in the model were updated, and the performance of the updated and former models in the prediction of ignition delay times (IDTs) was compared. Figure 6 shows the correlation of the IDTs obtained with closed batch homogeneous reactor simulations for the fuels shown in Table 2 using the updated and former thermochemistry data, on logarithmic scale (IDT data are provided as supplementary material). For each fuel, we obtained IDTs at 1 and 10 atm at different temperatures within the 700-1500 K range using increments of 200 K.

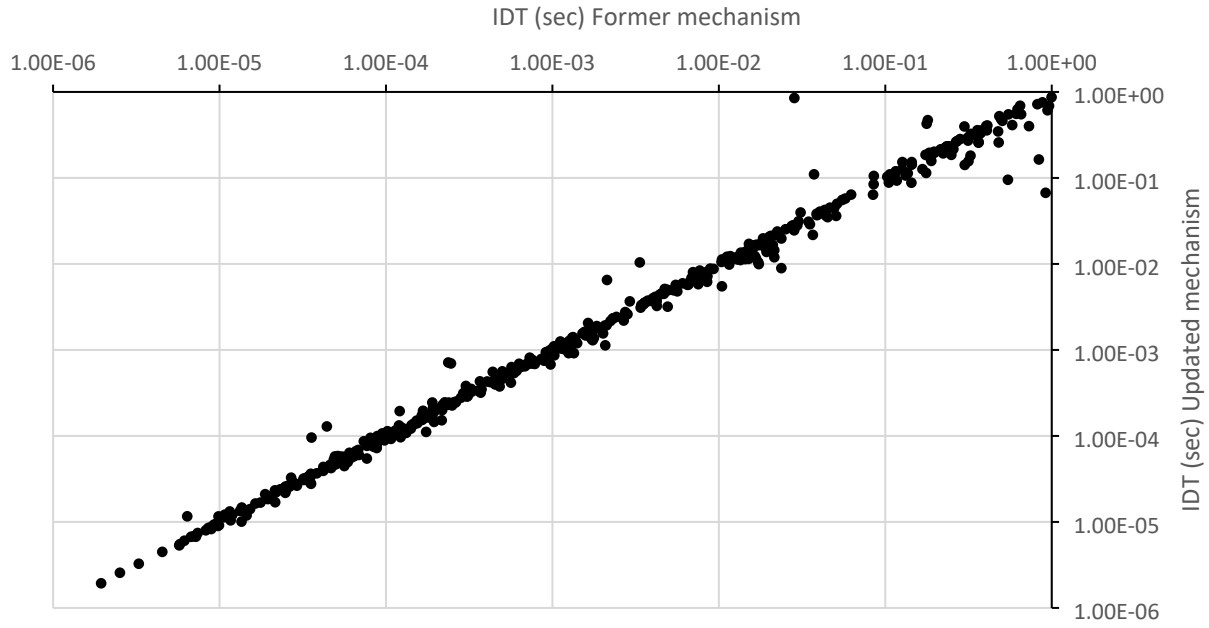

Figure 5: Comparison of the ignition delay times predicted by the former and updated kinetic models after the implementation of our calculated thermochemistry data.

The R-squared value is 0.55, which indicates that there is a notable effect on the performance of the chemical kinetic model when the thermochemistry is updated with our new values. The largest discrepancy is observed for the 2-methylhexane related species at 1 atm and 700K, for which the IDT with the original mechanism is 30 times lower than that predicted by the updated model. Large differences were also observed for 2,4,4-trimethylpent-1-ene and 2,4,4-trimethylpent-2-ene at 700 K and 10 atm. Note that the thermochemistry of RO radicals, which plays a crucial role in the ignition characteristics of hydrocarbons, is not updated for this comparison; however, GA

calculates their thermochemistry properties from those of the corresponding closed shell species, and since large uncertainties in entropy were observed for the latter, one can also expect the thermochemistry of those radicals to be uncertain and thus to affect the IDTs measurements as well as other important properties of the combustion system. This comparison highlights the importance of our updated dataset in order to improve kinetic models and the simulation of combustion systems.

4. Conclusions:

In this work, we ran electronic structure and statistical thermodynamic calculations to update the enthalpy of formation, entropy, and heat capacities of 1340 out of the 1368 closed shell species of the Co-optima mechanism. Electronic structure calculations were performed with the M06-2X/aug-cc-pVTZ and G3 levels of theory, and torsional anharmonicity was introduced by means of the hindered rotor approach and by scaling the vibrational frequencies. The thermochemistry data is also provided in the NASA polynomials format in the supplementary material, which can be readily used in kinetic modeling. This database also includes the corresponding rotational symmetry number and number of optical isomers of the species used for the calculations of thermochemistry.

To the author's knowledge, this is the largest and most accurate thermochemistry database for combustion kinetics modeling, with the following advantages and implications:

1) Our accurate thermochemistry database can be widely used to update different kinetic mechanisms of interest in combustion applications.

2) The consistency of the database makes it suitable for developing estimation models such as group additivity or machine-learning models.

3) Given the high accuracy of our database (mean absolute error of 0.34 kcal mol^{-1} for $\Delta_f H_{298}$), thermochemistry data can be left as a constrained variable during the optimization of kinetic models.

4) The discrepancies observed between the thermochemistry data reported in our database and that used in current kinetic models from less robust methodologies such as group additivity warrant a detailed assessment of the performance of those models and perhaps an update to them. In fact,

differences are observed between the updated and original Co-optima kinetic model in predicting ignition delay times for 59 different fuel components.

5) The M06-2X/aug-cc-pVTZ level of theory resulted in a relatively computationally expensive level given the size of the considered species and their large number of conformers, which difficult the optimization and characterization of the corresponding global minimum conformer. In fact, we estimate that the total cost of the electronic structure calculations that were ran for the optimization and characterization of the global minima (i.e. excluding the calculations for the conformational search) with the Gaussian16 software is about 10 million core hours in our Ibex supercomputer. We conclude that using a lower level of theory for the conformational search is convenient when one deals with large species that have complex conformational spaces, and also that the use of high level quantum chemistry methods is still prohibitive for such large datasets with complex species.

Acknowledgement

This work was supported by King Abdullah University of Science and Technology (KAUST) Office of Sponsored Research under the award number OSR-2019-CRG7-4077.

References

[1] Battin-Leclerc F, Simmie JM, Blurock E. Cleaner combustion. Dev Detail Chem Kinet Model Ser Green Energy Technol Cham Springer Int Publ AG 2013.

[2] Pedley JB, Naylor RD, Kirby SP. Thermochemical Data of Organic Compounds. Second Edition. Chapman & Hall London 1986.

[3] Rowley RL, Wilding WV, Oscarson JL, Yang Y, Zundel NA, Daubert TE, Danner RP. DIPPR® Data Compilation of Pure Compound Properties. Design Institute for Physical Properties. AIChE New York 2003.

[4] Yaws CL. Yaws' Handbook of Thermodynamic and Physical Properties of Chemical Compounds. Knovel, Norwich, NY 2003.

[5] Baulch DL, Bowman CT, Cobos CJ, Cox RA, Just T, Kerr JA, et al. Evaluated kinetic data for combustion modeling: supplement II. J Phys Chem Ref Data 2005;34:757–1397.

[6] CRC Handbook of Chemistry and Physics, 2009−2010, 90th ed. J Am Chem Soc

2009;131:12862.

[7] Frenklach M, Packard A, Djurisic ZM, Golden DM, Bowman CT, Green WH, et al. PrIMe: Process Informatics Model, 2007.

[8] Goos E, Burcat A, Ruscic B. Extended third millennium ideal gas and condensed phase thermochemical database for combustion with updates from active thermochemical tables. Elke Goos, Remchingen, Ger Accessed Sept 2010;19:2016.

[9] Linstrom PJ, Mallard WG. NIST Chemistry WebBook. National Institute of Standards and Technology. Gaithersburg MD, 20899. http://webbook.nist.gov

[10] Ruscic B, Pinzon RE, Laszewski G von, Kodeboyina D, Burcat A, Leahy D, et al. Active Thermochemical Tables: thermochemistry for the 21st century. J Phys Conf Ser 2005;16:561–70.

[11] Goldsmith CF, Magoon GR, Green WH. Database of Small Molecule Thermochemistry for Combustion. J Phys Chem A 2012;116:9033–57.

[12] Ghahremanpour MM, van Maaren PJ, Ditz JC, Lindh R, van der Spoel D. Large-scale calculations of gas phase thermochemistry: Enthalpy of formation, standard entropy, and heat capacity. J Chem Phys 2016;145:114305.

[13] Li Y, Curran HJ. Extensive Theoretical Study of the Thermochemical Properties of Unsaturated Hydrocarbons and Allylic and Super-Allylic Radicals: The Development and Optimization of Group Additivity Values. J Phys Chem A 2018;122:4736–49.

[14] Bugler J, Somers KP, Silke EJ, Curran HJ. Revisiting the kinetics and thermodynamics of the low-temperature oxidation pathways of alkanes: a case study of the three pentane isomers. J Phys Chem A 2015;119:7510–27.

[15] Hudzik JM, Bozzelli JW, Simmie JM. Thermochemistry of C7H16 to C10H22 alkane isomers: primary, secondary, and tertiary C--H bond dissociation energies and effects of branching. J Phys Chem A 2014;118:9364–79.

[16] Hudzik JM, Bozzelli JW. Thermochemistry of hydroxyl and hydroperoxide substituted furan, methylfuran, and methoxyfuran. J Phys Chem A 2017;121:4523–44.

[17] Hudzik JM, Bozzelli JW. Thermochemistry and bond dissociation energies of ketones. J Phys Chem A 2012;116:5707–22.

[18] Snitsiriwat S, Bozzelli JW. Thermochemical properties for isooctane and carbon radicals: Computational study. J Phys Chem A 2013;117:421–9.

[19] Yommee S, Bozzelli JW. Cyclopentadienone oxidation reaction kinetics and thermochemistry for the alcohols, hydroperoxides, and vinylic, alkoxy, and alkylperoxy radicals. J Phys Chem A 2016;120:433–51.

[20] Chen C-C, Bozzelli JW, Krasnoperov LN. Thermochemical Properties of Hydroxycyclohexadienyl Peroxy Isomers from Reaction of O2 with the Benzene-OH adduct. Zeitschrift Für Phys Chemie 2015;229:999–1036.

[21] Auzmendi-Murua I, Bozzelli JW. Thermochemical Properties and Bond Dissociation Energies of C3--C5 Cycloalkyl Hydroperoxides and Peroxy Radicals: Cycloalkyl Radical+ 3O2 Reaction Thermochemistry. J Phys Chem A 2012;116:7550–63.

[22] Yalamanchi KK, Monge-Palacios M, van Oudenhoven VCO, Gao X, Sarathy SM. Data Science Approach to Estimate Enthalpy of Formation of Cyclic Hydrocarbons. J Phys Chem A 2020;124:6270–6.

[23] Yalamanchi KK, van Oudenhoven VCO, Tutino F, Monge-Palacios M, Alshehri A, Gao X, et al. Machine Learning To Predict Standard Enthalpy of Formation of Hydrocarbons. J Phys Chem A 2019;123:8305–13.

[24] Aldosari MN, Yalamanchi KK, Gao X, Sarathy SM. Predicting entropy and heat capacity of hydrocarbons using machine learning. Energy AI 2021;4:100054.

[25] Mehl M, Wagnon S, Tsang K, Kukkadapu G, Pitz WJ, Westbrook CK, et al. A comprehensive detailed kinetic mechanism for the simulation of transportation fuels. 10th US National Combustion Meeting.

[26] Cheng S, Saggese C, Kang D, Goldsborough SS, Wagnon SW, Kukkadapu G, et al. Autoignition and preliminary heat release of gasoline surrogates and their blends with ethanol at engine-relevant conditions: Experiments and comprehensive kinetic modeling. Combust Flame 2021;228:57–77.

[27] Zhao Y, Truhlar DG. The M06 suite of density functionals for main group thermochemistry, thermochemical kinetics, noncovalent interactions, excited states, and transition elements: two new functionals and systematic testing of four M06-class functionals and 12 other function. Theor Chem Acc 2008;120:215–41.

[28] Kendall RA, Dunning TH, Harrison RJ. Electron affinities of the first-row atoms revisited. Systematic basis sets and wave functions. J Chem Phys 1992;96:6796–806.

[29] Montgomery JA, Frisch MJ, Ochterski JW, Petersson GA. A complete basis set model chemistry. VII. Use of the minimum population localization method. J Chem Phys 2000;112:6532–42.

[30] Curtiss LA, Raghavachari K, Redfern PC, Rassolov V, Pople JA. Gaussian-3 (G3) theory for molecules containing first and second-row atoms. J Chem Phys 1998;109:7764–76.

[31] Curtiss LA, Redfern PC, Raghavachari K. Gaussian-4 theory. J Chem Phys 2007;126:84108.

[32] Dong S, Wagnon SW, Pratali Maffei L, Kukkadapu G, Nobili A, Mao Q, et al. A new detailed kinetic model for surrogate fuels: C3MechV3.3. Appl Energy Combust Sci 2022;9:100043.

[33] Chai J-D, Head-Gordon M. Long-range corrected hybrid density functionals with damped atom--atom dispersion corrections. Phys Chem Chem Phys 2008;10:6615–20.

[34] Ditchfield R, Hehre WJ, Pople JA. Self-consistent molecular-orbital methods. IX. An extended Gaussian-type basis for molecular-orbital studies of organic molecules. J Chem Phys 1971;54:724–8.

[35] Clark T, Chandrasekhar J, Spitznagel GW, Schleyer PVR. Efficient diffuse function-augmented basis sets for anion calculations. III. The 3-21+ G basis set for first-row elements, Li--F. J Comput Chem 1983;4:294–301.

[36] Simmie JM, Somers KP. Benchmarking compound methods (CBS-QB3, CBS-APNO, G3, G4, W1BD) against the active thermochemical tables: a litmus test for cost-effective molecular formation enthalpies. J Phys Chem A 2015;119:7235–46.

[37] Somers KP, Simmie JM. Benchmarking compound methods (CBS-QB3, CBS-APNO, G3, G4, W1BD) against the active thermochemical tables: formation enthalpies of radicals. J Phys Chem A 2015;119:8922–33.

[38] Frisch MJ, Trucks GW, Schlegel HB, Scuseria GE, Robb M a., Cheeseman JR, et al. G16_C01 2016:Gaussian 16, Revision C.01, Gaussian, Inc., Wallin.

[39] Wavefunction, Inc. Spartan'18 version 1.4.5 (Irvine, CA).

[40] Barker JR. Multiple-Well, multiple-path unimolecular reaction systems. I. MultiWell computer program suite. Int J Chem Kinet 2001;33:232–45.

[41] Alecu IM, Zheng J, Zhao Y, Truhlar DG. Computational thermochemistry: scale factor databases and scale factors for vibrational frequencies obtained from electronic model chemistries. J Chem Theory Comput 2010;6:2872–87.